The cytomegalovirus-encoded chemokine receptor US28 promotes intestinal neoplasia in transgenic mice

Gerold Bongers,[1] David Maussang,[1,2] Luciana R. Muniz,[1] Vanessa M. Noriega,[3] Alberto Fraile-Ramos,[4] Nick Barker,[5] Federica Marchesi,[1] Nanthakumar Thirunarayanan,[1] Henry F. Vischer,[2] Lihui Qin,[6] Lloyd Mayer,[1] Noam Harpaz,[6] Rob Leurs,[2] Glaucia C. Furtado,[1] Hans Clevers,[5] Domenico Tortorella,[3] Martine J. Smit,[2] and Sergio A. Lira[1]

[1]Immunology Institute, Mount Sinai School of Medicine, New York, New York, USA. [2]Leiden/Amsterdam Center for Drug Research, Department of Medicinal Chemistry, Vrije Universiteit Amsterdam, Amsterdam, The Netherlands. [3]Department of Microbiology, Mount Sinai School of Medicine, New York, New York, USA. [4]Cell Biology Unit, Medical Research Council Laboratory for Molecular Cell Biology, University College London, London, United Kingdom. [5]Hubrecht Institute, Koninklijke Nederlandse Akademie van Wetenschappen, and University Medical Center Utrecht, Utrecht, The Netherlands. [6]Division of Gastrointestinal Pathology, Department of Pathology, The Mount Sinai Medical Center, New York, New York, USA.

US28 is a constitutively active chemokine receptor encoded by CMV (also referred to as human herpesvirus 5), a highly prevalent human virus that infects a broad spectrum of cells, including intestinal epithelial cells (IECs). To study the role of US28 in vivo, we created transgenic mice (*VS28* mice) in which US28 expression was targeted to IECs. Expression of US28 was detected in all IECs of the small and large intestine, including in cells expressing leucine rich repeat containing GPCR5 (*Lgr5*), a marker gene of intestinal epithelial stem cells. US28 expression in IECs inhibited glycogen synthase 3β (GSK-3β) function, promoted accumulation of β-catenin protein, and increased expression of Wnt target genes involved in the control of the cell proliferation. *VS28* mice showed a hyperplastic intestinal epithelium and, strikingly, developed adenomas and adenocarcinomas by 40 weeks of age. When exposed to an inflammation-driven tumor model (azoxymethane/dextran sodium sulfate), *VS28* mice developed a significantly higher tumor burden than control littermates. Transgenic coexpression of the US28 ligand CCL2 (an inflammatory chemokine) increased IEC proliferation as well as tumor burden, suggesting that the oncogenic activity of US28 can be modulated by inflammatory factors. Together, these results indicate that expression of US28 promotes development of intestinal dysplasia and cancer in transgenic mice and suggest that CMV infection may facilitate development of intestinal neoplasia in humans.

Introduction

Human CMV (also know as human herpesvirus 5 [HHV-5]) infects millions of people worldwide (50%–90% of the population is seropositive for CMV antigens). Primary infection of immunocompetent hosts with CMV is generally asymptomatic and persistent but may cause severe disease in immunodeficient hosts, such as developing fetuses, transplant recipients, and AIDS patients (1). In fact, CMV is the most common viral opportunistic infection in people with AIDS. Individuals infected with CMV mount a strong immune response that suppresses persistent viral replication and maintains life-long latency; however, loss of immune control permits viral reactivation and disease (2).

The 230-kbp genome of CMV encodes for about 200 genes, including the GPCRs *US27*, *US28*, *UL33*, and *UL78* (3). US28 shares highest sequence homology with human chemokine receptors (4) and binds several chemokines, including CCL2, CCL3, CCL4, CCL5, and CX_3CL1 (5, 6). Unlike most chemokine receptors that couple predominantly to $G\alpha_{i/o}$ proteins, US28 promiscuously couples to $G\alpha_{i/o}$, $G\alpha_{16}$, $G\alpha_{12/13}$, and $G\alpha_q$ proteins (7). Consequently, US28 activates many different signal transduction pathways. US28 constitutively activates PLC and thereby increases intracellular inositol trisphosphate. Moreover, US28 constitutively activates NF-κB, the cAMP response element-binding protein (CREB), and nuclear factor of activated T cells (NFAT) (7). The constitutive activity of US28 can be regulated by chemokines. Stimulation of US28-transfected cells with CCL2, CCL3, and CCL5 increases intracellular calcium and ERK phosphorylation in a $G\alpha_{i/o}$ and $G\alpha_{16}$ protein–dependent manner. The constitutive activity of US28 can be inhibited by its inverse agonist CX_3CL1 and by the small molecular weight compound VUF2274 (7, 8).

In vitro infection with CMV leads to expression of US28 during the immediate-early and latent phase of viral cycle (9, 10). Several functions have been suggested for US28, including sequestration of chemokines (11, 12) and enhancement of cell-cell interactions (13). US28 has also been shown to induce chemokinesis when transfected into smooth muscle cells but not when transfected into fibroblasts. Likewise, expression of US28 in HEK293T, COS-7, and HELA cells results in caspase 8– and 10–mediated apoptosis (14). A function attributed more recently to US28 is the induction of neoplasia. Stable expression of US28 in NIH-3T3 cells leads to enhanced cell cycle progression and loss of contact inhibition. Injection of such cells into nude mice induces the formation of tumors, suggesting that US28 may have oncogenic properties (15).

CMV can infect a broad spectrum of cells in the gastrointestinal tract (16). CMV infection has been detected in colonic epithelial

Authorship note: Gerold Bongers and David Maussang contributed equally to this work.

Conflict of interest: The authors have declared that no conflict of interest exists.

Citation for this article: *J Clin Invest.* 2010;120(11):3969–3978. doi:10.1172/JCI42563.

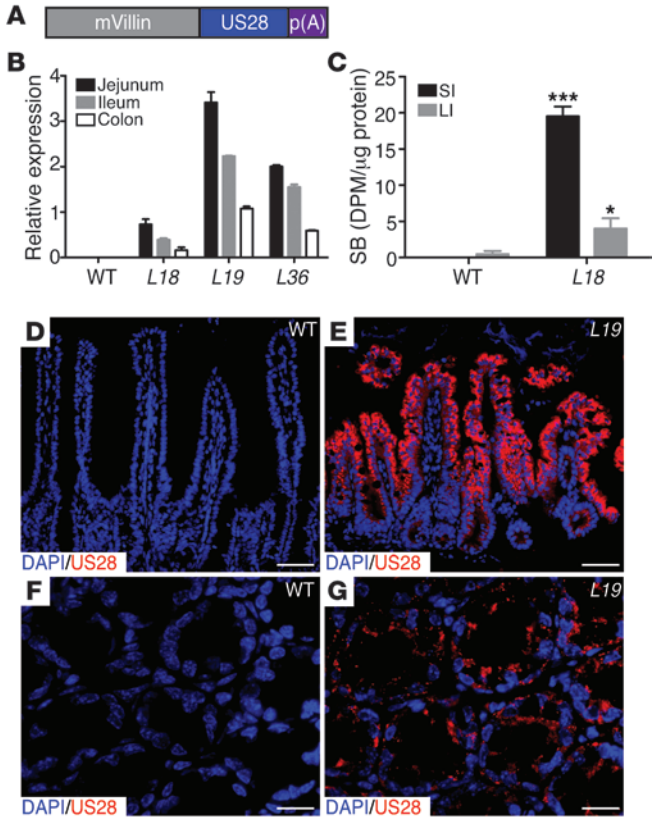

Figure 1
Expression of the US28 transgene in *VS28* mice. (**A**) Diagram of the *VS28* transgene. Expression of US28 is driven by the 9-kb mouse villin promoter (mVillin). (**B**) *US28* mRNA expression in jejunum, ileum, and colon of WT, *VS28*^{L18}, *VS28*^{L19}, and *VS28*^{L36} mice. Values were standardized to ubiquitin. Results represent the mean ± SEM (n = 3–4). (**C**) Radioligand competition assay using [^{125}I]-CCL5 on membranes of IECs isolated from of the small intestine (SI) or large intestine (LI) of WT or *VS28*^{L18} mice. Results are expressed as specific binding (SB) in disintegrations per minute (DPM) divided by total protein. Results represent the mean ± SEM (n = 3). *P < 0.05, ***P < 0.001 vs. WT. (**D**–**G**) Representative images of the jejunum (**D** and **E**) and colon (**F** and **G**) of WT (**D** and **F**) and *VS28*^{L19} (**E** and **G**) mice stained with US28 (red) and DAPI (blue). Scale bar: 50 μm (**D** and **E**); 25 μm (**F** and **G**).

cells of immunocompromised patients (17, 18) as well as immunocompetent individuals (19). To date, all information regarding the physiological importance of US28 is based on in vitro models. To determine the role of US28 in vivo, we constructed strains of mice in which expression of US28 was targeted to intestinal epithelial cells (IECs), including intestinal epithelial stem cells, as defined by expression of the marker gene leucine rich repeat containing GPCR5 (*Lgr5*) (20). We show here that expression of US28 in the intestine of transgenic mice promotes development of intestinal neoplasia.

Results

Generation of mice expressing US28 in IECs. To investigate the biological role of the US28 in the IECs in vivo, we generated transgenic mice that express US28 under the control of the villin promoter (*VS28* mice) (Figure 1A). The villin promoter has been previously shown to target transgene expression predominately to the IECs of both the small and large intestine (21). Eleven founders were generated from microinjection of the US28 transgene into fertilized mouse eggs. Three transgenic lines (L18, L19, and L36) were established from these founders. Expression of US28 was determined by quantitative PCR (qPCR). *US28* mRNA was detected in all 3 transgenic lines but not in WT controls. The highest expression of *US28* mRNA was found in the jejunum, followed by the ileum and the colon of animals in line 19 (Figure 1B). To examine whether US28 protein was present in epithelial membranes, we performed radioligand competition binding experiments. As expected, human [^{125}I]-CCL5 did not bind to IEC membranes derived from WT mice. In contrast, human [^{125}I]-CCL5 bound to IEC membranes isolated from the small and large intestine of *VS28* mice. The specific binding of human [^{125}I]-CCL5 was higher (3 fold) in the small intestine than in the large intestine of *VS28* mice (Figure 1C), correlating well with the qPCR data (Figure 1B). To examine distribution of US28 protein in the intestine, we performed immunostaining with a US28 antibody. US28 expression was detected in IECs of transgenic but not WT mice (Figure 1, D and E). The staining was observed in cells in the villi and crypts throughout the intestine. Together, these results indicate that *VS28* mice express US28 in the intestinal epithelium.

US28 expression promotes phenotypic changes in the intestinal epithelium. To analyze whether expression of US28 promoted changes in the intestinal epithelium, we examined H&E-stained sections from *VS28* mice. Microscopically, the jejunal mucosae of all lines featured markedly hyperplastic nonmucinous villous epithelium, characterized by pseudostratified columnar cells forming tufts and floret-like configurations along the villous surfaces (Figure 2, A and B). Goblet cells were not increased. Apoptotic bodies were scattered within the villous epithelium. These abnormalities gradually

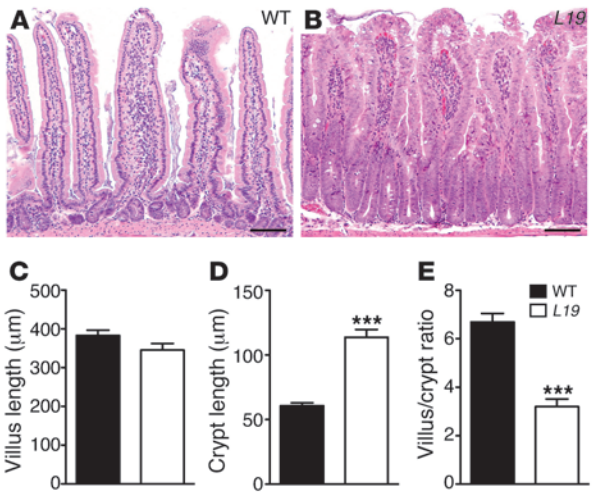

Figure 2
Histological changes in *VS28* mice. (**A** and **B**) H&E staining of the jejunum of WT (**A**) and *VS28*^{L19} mice (**B**). Scale bar: 100 μm. (**C**–**E**) Decreased villus length (**C**) and increased crypt size (**D**) in *VS28*^{L19} mice compared with those of WT mice. (**E**) Correspondingly, the villus/crypt ratio is decreased in *VS28*^{L19} mice compared with that of WT. On average, 80 crypts were measured for each mouse. Results represent the mean ± SEM (n = 12 mice per group). ***P < 0.001 vs. WT.

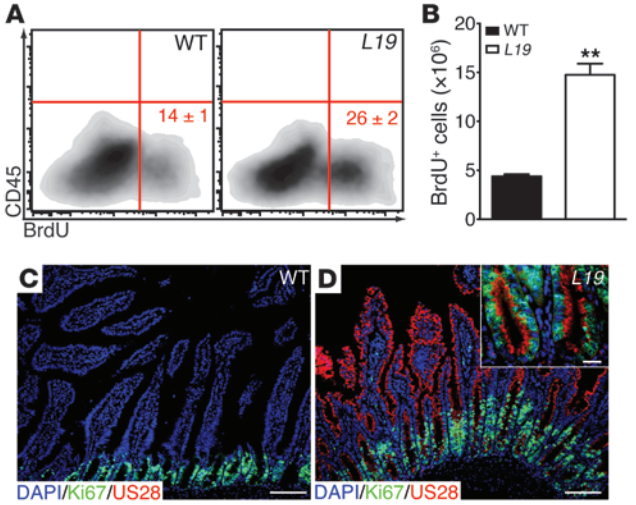

Figure 3
US28 expression induces IEC proliferation. (**A** and **B**) FACS analysis showing a relative (**A**) and absolute (**B**) increase of BrdU-positive CD45⁻ IECs from the jejunum of *VS28*^{L19} mice compared with those of WT littermates. Numbers indicate the percentage of BrdU⁺ cells. Results represent the mean ± SEM (n = 3 mice per group). $^{**}P < 0.01$ vs. WT mice. (**C** and **D**) Increased Ki67-positive cells in *VS28*^{L19} mice (**D**) compared with those in WT mice (**C**). The inset shows a high magnification of intestinal crypts and reveals expression of US28 in Ki67⁺ cells. Staining of the jejunum with DAPI (blue), US28 (red), and Ki67 (green). Scale bar: 100 μm (**C** and **D**); 25 μm (**D**, inset).

dissipated toward the ileum. In *VS28*^{L18} mice, the villus/crypt ratio was normal (5:1). The nuclei, albeit stratified, were of normal size and appearance, and the villi contained relatively fewer apoptotic bodies. The villus/crypt ratio in *VS28*^{L19} and *VS28*^{L36} mice ranged from 3:1 to 2:1, due to doubling of the crypt height (Figure 2). The nuclei were enlarged and contained prominent, enlarged nucleoli and thick nuclear membranes. The colonic mucosa of *VS28*^{L19} and *VS28*^{L36} mice featured crypts distended by hyperplastic epithelium, arranged in pseudostratified and pseudocribriform formations and extending to the surface, whereas that of *VS28*^{L18} mice was normal. Together, these results indicate that US28 promotes dose-dependent changes in the epithelium of both small and large intestine of transgenic mice.

US28 expression promotes IEC proliferation. To determine whether the changes reported above were due to increased proliferation of IECs, we examined BrdU incorporation using flow cytometry. The number of BrdU-positive IECs was significantly higher in *VS28*^{L19} mice than in WT littermates (Figure 3, A and B). To confirm these results, we analyzed the expression of the cell proliferation marker Ki67 by immunostaining. In the intestine of WT mice, Ki67 expression was frequently detected in cells in the crypts and rarely detected in cells within the lamina propria (Figure 3C). This pattern was also observed in the transgenic sections, but the number of Ki67⁺ cells in the crypts was markedly increased compared with that of WT mice (Figure 3D). Importantly, most cells coexpressed US28 and Ki67 (Figure 3D, inset). Together, these results indicate that the expression of US28 in IECs induces marked cell proliferation.

US28 expression affects pathways implicated in IEC proliferation. To determine the mechanism by which US28 mediates increased proliferation of IECs, we investigated 2 pathways that are important for the regulation of IEC proliferation: the Wnt and the MAPK pathways (22, 23).

Activation of Wnt signaling leads to the activation of downstream effectors, ultimately promoting accumulation of β-catenin protein (24). To determine whether activation of the Wnt pathway plays a role in the increased proliferation of IECs observed in *VS28* mice, we determined mRNA and protein levels of β-catenin. The protein levels of β-catenin were increased 13 fold in IECs isolated from the small intestine of the *VS28*^{L19} mice compared with those of WT (Figure 4B). No significant difference was found between β-catenin (*Ctnnb1*) mRNA levels in IECs isolated from WT or *VS28*^{L19} mice, indicating that regulation of β-catenin occurred at the protein level rather than at the transcriptional level.

GPCRs regulate β-catenin protein levels via GSK-3β (25). In the absence of GPCR/Wnt signaling, GSK-3β phosphorylates

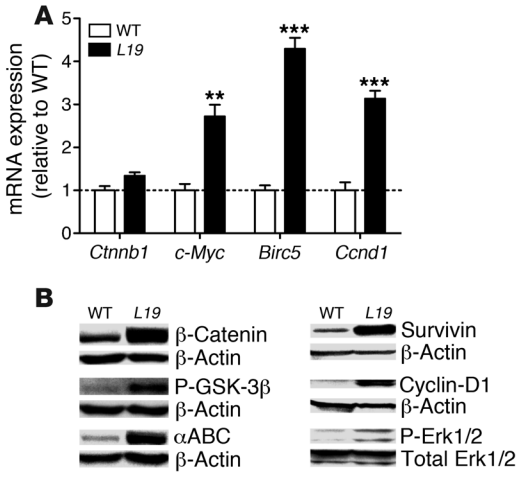

Figure 4
Expression of US28 in IECs leads to activation of Wnt and MAPK pathways. (**A**) Increased mRNA levels of the Wnt target genes *c-myc*, *Birc5*, and *Ccnd1* in IECs from *VS28*^{L19} mice. Notice that the mRNA levels of *Ctnnb1* were not changed. The dashed line indicates WT values. Values were standardized to ubiquitin Results represent the mean ± SEM (n = 3–4 mice per group). $^{**}P < 0.01$, $^{***}P < 0.001$ vs. WT. (**B**) Western blot analysis of total β-catenin, phosphorylated GSK-3β/Ser^{9}, active non-phosphorylated β-catenin (αABC), cyclin-D1, survivin, and phosphorylated Erk1/2 in IECs from *VS28*^{L19} and WT mice. A representative blot is show of from 3 independent experiments (n = 4).

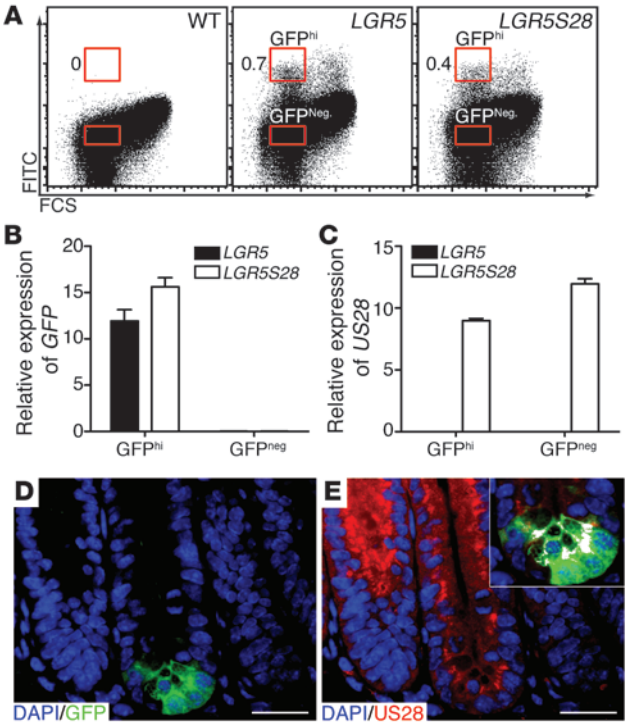

Figure 5
US28 is expressed in Lgr5+ intestinal stem cells. (**A**) GFP^{hi} and GFP^{neg} IECs were sorted from *LGR5* and *LGR5S28* mice. Numbers indicate the percentage of GFP^{hi} IECs. (**B** and **C**) *GFP* (**B**) and *US28* (**C**) mRNA expression in sorted cells from the small intestine of *LGR5* and *LGR5S28* mice. Values were standardized to ubiquitin. Results represent the mean ± SEM (n = 3). (**D** and **E**) US28 is expressed in Lgr5+ (GFP) cells. Staining of the jejunum of *LGR5S28* mice with DAPI (blue), US28 (red), and GFP (green). The inset shows colocalization of US28 in Lgr5+ cells in white. Scale bar: 25 μm (**D** and **E**).

β-catenin, which leads to its degradation. Phosphorylation of GSK-3β leads to its inactivation and results in increased levels of active, unphosphorylated β-catenin. To evaluate whether modulation of GSK-3β plays a role in the increased levels of β-catenin, we evaluated the phosphorylation status of GSK-3β at Ser^9 and of β-catenin. We found that the phosphorylation of GSK-3β was increased and that the total amount of active, unphosphorylated β-catenin protein was increased (Figure 2B).

To test whether increased levels of active β-catenin had functional consequences, we examined expression of the Wnt target genes *c-myc*, survivin (*Birc5*), and cyclin-D1 (*Ccnd1*) in IECs isolated from WT and *VS28^{L19}* mice. The mRNA levels of *c-myc*, *Birc5*, and *Ccnd1* were significantly increased in *VS28^{L19}* mice (Figure 4A). To confirm these changes, we determined the protein levels of survivin and cyclin-D1 by Western blotting. We found that the protein levels of survivin and cyclin-D1 were elevated in IECs purified from *VS28^{L19}* mice compared with those of WT mice (Figure 4B).

In NIH-3T3 cells, stable expression of US28 leads to increased transcription of genes downstream of the MAPK pathway (26). To test whether US28 modulates MAPK signaling in *VS28* mice, we analyzed the amount of Erk1/2 phosphorylation in purified IECs by Western blotting. Our results show that the amount of phosphorylated Erk1/2 was increased 2.6 fold in the *VS28^{L19}* mice compared with WT littermates, whereas total levels of Erk1/2 were unaffected (Figure 4B). Together, these results indicate that expression of US28 promotes marked changes in the activation of the Wnt and MAPK pathways and suggest that these pathways are mechanistically implicated in the increased cellular proliferation of IECs observed in *VS28* mice.

US28 is expressed in Lgr5+ intestinal stem cells. Accumulation of β-catenin in intestinal stem cells appears to be a key mechanism driving epithelial cell proliferation (27). Thus, the increased cell proliferation observed in the *VS28* mice may have been due to expression of US28 in the stem cell compartment. It has been recently reported that the cells expressing Lgr5 are the intestinal stem cells (20). To test whether US28 was expressed in Lgr5+ cells, we took advantage of the *Lgr5-EGFP-IRES-creERT2* (*LGR5*) mice (20), which have the *gfp* gene inserted in the *Lgr5* locus. We crossed *LGR5* mice with *VS28^{L36}* mice to generate *LGR5S28* mice. IECs were isolated from *LGR5* and *LGR5S28* mice and sorted. Both GFP^{hi} and GFP-negative (GFP^{neg}) cells were sorted (Figure 5A) and analyzed by qPCR for expression of GFP and US28. As expected, no *US28* mRNA was detected in stem cells (GFP^{hi} cells) from *LGR5* mice. *US28* mRNA was detected in stem cells from LGRS28 mice, although at lower levels than those found in other epithelial cells (GFP^{neg} cells). (Figure 5, B and C). To confirm these findings, we stained jejunal sections of *LGR5S28* mice for US28 and GFP. Similar to the qPCR results, US28 was found to be expressed in Lgr5+ cells (Figure 5, D and E). These results indicate that US28 is expressed in Lgr5+ intestinal stem cells of *VS28* mice.

Long-term expression of US28 induces the development of colon cancer. To examine the long-term consequences of US28 expression in IECs, we examined *VS28^{L18}*, *VS28^{L19}*, and *VS28^{L36}* mice at different ages. Before 39 weeks of age no microscopic abnormalities were observed, other than those previously described (n = 22). However, beginning at 39 weeks intestinal neoplasms developed in 17 out of 105 *VS28* mice in all 3 lines but not in their WT littermates (n = 50). Tumors were most frequent in the *VS28^{L19}* line, which had the highest level of US28 expression (10 out of 25 mice, 40%; $P < 0.001$ compared with WT), followed by the *VS28^{L36}* line (3 out of 12 mice, 25%; $P < 0.01$ compared with WT) and the *VS28^{L18}* line (4 out of 49 mice, 8.2%; $P < 0.1$ compared with WT). Besides increased tumor penetrance, the 2 lines with the highest levels of expression also had an increased average tumor multiplicity (2.2 ± 0.5, 2.0 ± 0.6, and 1.3 ± 0.3 tumors per mouse in lines *VS28^{L19}*, *VS28^{L36}*, and *VS28^{L18}*, respectively) (Table 1).

In total, 2 moderately to poorly differentiated colonic adenocarcinomas were found in 1 mouse, 1 tubular adenocarcinoma was found in another mouse, and 27 adenomas (26 jejunal and

Table 1
Prevalence of neoplasms in *VS28* mice

Mice	Age (wk)	Adenocarcinoma	Adenoma	Multiplicity
WT	40–65	(0/50) 0%	(0/50) 0%	N/A
VS28^{L18}	39–64	(1/49) 2%	(3/49) 6%	1.3 ± 0.3
VS28^{L19}	40–68	(1/25) 4%	(9/25) 36%^{A,B}	2.2 ± 0.5
VS28^{L36}	40–43	(0/12) 0%	(3/12) 25%^{C}	2.0 ± 0.6

Mice (39–68 weeks of age) were examined for the presence of intestinal neoplasia. $^{A}P < 0.001$ vs. WT. $^{B}P < 0.01$ vs. *VS28^{L18}*. $^{C}P < 0.01$ vs. WT. N/A, not applicable.

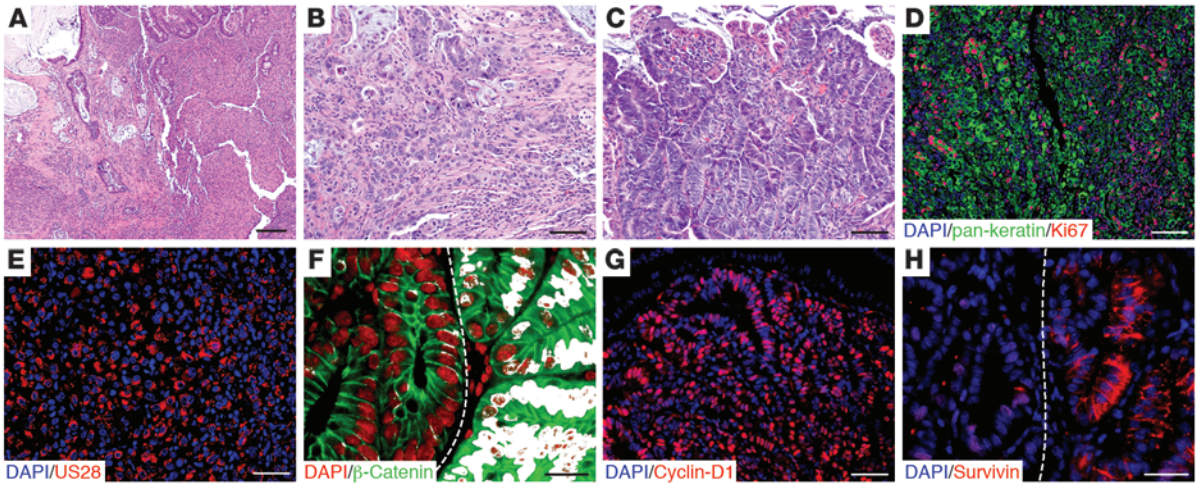

Figure 6
Colonic and jejunal tumors in *VS28* mice. (**A** and **B**) H&E-stained sections of a poorly differentiated colon carcinoma found in a *VS28*^{L18} mouse at 42 weeks of age. (**C**) H&E-stained section of jejunal tubular adenoma with high-grade dysplasia found in a *VS28*^{L19} mouse. (**D** and **E**) Tumors found in *VS28* mice are positive for pan-keratin, Ki67 (**D**), and US28 (**E**). Representative sections stained with DAPI (blue), pan-keratin (**D**, green), Ki67 (**D**, red), or US28 (**E**, red) are shown. (**F**) β-catenin is present in the nucleus (white) of an adenoma (right side of the dashed line) of a *VS28*^{L19} mouse. No nuclear translocation is seen in normal crypts (left side of the dashed line). Representative sections stained with DAPI (red) and β-catenin (green) are shown. Nuclear translocation (double staining) is indicated in white. (**G**) Jejunal adenomas express cyclin-D1. A representative section stained with DAPI (blue) and cyclin-D1 (red) is shown. (**H**) Survivin was found in the cytosol of jejunal tubular adenomas (right side of the dashed line), in contrast to its normal nuclear localization (left side of the dashed line). Scale bar: 200 μm (**A**); 100 μm (**B**–**D**); 50 μm (**E** and **G**); 20 μm (**F** and **H**).

1 colonic) were found in 15 mice (Table 1). The moderately to poorly differentiated adenocarcinomas featured sheets and glands of malignant epithelium with areas of mucin secretion. Both lesions invaded the pericolonic subserosa but had not metastasized (Figure 6, A–C). The cancer cells expressed cytokeratin, Ki67 (Figure 6D), and US28 (Figure 6E) but were negative for CD117, smooth muscle actin, and CD68. The adenocarcinomas featured low- and high-grade dysplasia, with glands invading into the submucosa. The other tumors were sessile tubular adenomas (12 with high-grade dysplasia and 15 with low-grade dysplasia).

Immunostaining of the adenomas with high-grade dysplasia further confirmed an association of US28 expression and aberrant Wnt signaling. In all adenomas tested (n = 4), β-catenin was ectopically distributed. β-Catenin was frequently found in the nucleus of neoplastic cells, in contrast to the normal surrounding cells, which exhibited localization of β-catenin in the cytoplasm (Figure 6F). Additionally, the adenomas expressed the protooncogene cyclin-D1, a target of β-catenin (Figure 6G). Changes were also observed in the cellular localization of survivin. In the adenomas, survivin expression was detected focally in the cytoplasm rather than in the nucleus (Figure 6H). These results indicate that expression of US28 in IECs leads to the development of neoplastic lesions that show evidence of aberrant Wnt signaling.

US28 expression alters susceptibility to colitis-associated neoplasia. Having observed that intestinal neoplasms developed spontaneously after approximately 39 weeks of age, we next asked whether US28 signaling could affect development of neoplasia promoted by inflammatory stimuli. To this end, we used a well-established protocol to induce colitis-associated neoplasia, the azoxymethane/

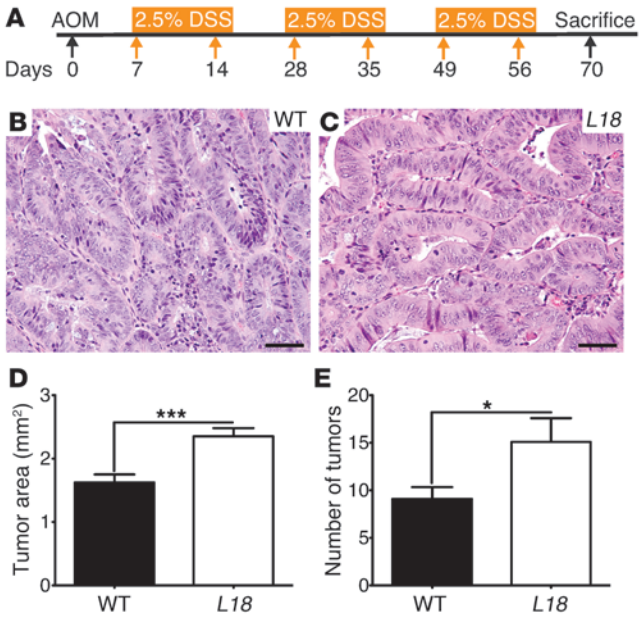

Figure 7
Response of *VS28* and WT mice to AOM/DSS. (**A**) Schematic of AOM/DSS administration. Mice were injected with 12 mg/kg AOM and subjected to three 7-day cycles of 2.5% DSS. (**B** and **C**) Representative H&E-stained sections of adenomas found after AOM/DSS treatment in WT (**B**) and *VS28*^{L18} mice (**C**). Scale bar: 50 μm. (**D** and **E**) The number of polyps (**E**) and the polyp area (**D**) were significantly increased in the *VS28*^{L18} mice (n = 11) compared with those of the WT littermates (n = 11). Results represent the mean ± SEM. *P < 0.05, ***P < 0.001 vs. WT.

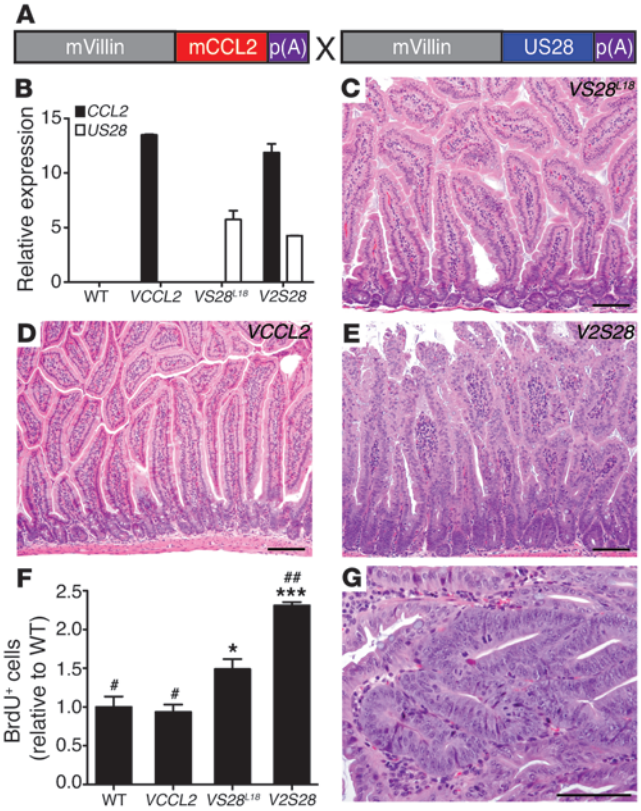

Figure 8
Transgenic coexpression of the inflammatory chemokine CCL2 exacerbates the phenotype of *VS28*^{L18} mice. The inflammatory chemokine CCL2 is an agonist for US28. To test whether CCL2 can activate US28 in vivo, we generated mice expressing both CCL2 and US28 in IECs. (**A**) Generation of mice expressing both CCL2 and US28 in IECs (*V2S28* mice). A 9-kb fragment of the villin promoter was used to drive expression of mouse CCL2 (mCCL2) to IECs (*VCCL2* mice). Subsequently, the *VCCL2* transgenic mice were crossed with *VS28*^{L18} mice to generate *V2S28* mice. (**B**) *CCL2* and US28 mRNA expression in the jejunum of WT, *VCCL2*, *VS28*^{L18}, and *V2S28* mice. Values were standardized to ubiquitin (n = 3). (**C**–**E**) H&E staining of the jejunum of *VS28*^{L18} (**C**), *VCCL2* (**D**), and *V2S28* mice (**E**). (**F**) Analysis of BrdU$^+$ incorporation in CD45$^-$ IECs from the jejunum of WT, *VCCL2*, *VS28*^{L18}, and *V2S28* mice was determined using FACS analysis (n = 4 mice per group). $^*P < 0.05$, $^{***}P < 0.001$ vs. WT. $^{\#}P < 0.05$, $^{\#\#}P < 0.01$ vs. *VS28*^{L18}. (**G**) H&E-stained section of jejunal tubular adenoma found in a *V2S28* mouse. Scale bar: 100 μm (**C**–**E** and **G**). Results represent the mean ± SEM.

dextran sodium sulfate model (AOM/DSS model) (28). *VS28*^{L18} mice (n = 11) and their age- and sex-matched WT littermates (n = 11) were treated with 3 repeated cycles of 2.5% DSS after AOM injection (12 mg/kg, i.p.) (Figure 7A). At the end of treatment, both transgenic and control mice manifested colonic adenomas (Figure 7, B and C). However, *VS28* mice had higher tumor multiplicity and larger area than their control littermates (Figure 7, D and E). These results suggest that US28 expression exacerbated the development of tumors induced by the AOM/DSS treatment.

Coexpression of the inflammatory chemokine CCL2 exacerbates phenotype of VS28^{L18} *mice*. US28 is most homologous to human chemokine receptors (4) and binds several inflammatory chemokines. The high constitutive activity of US28 can be further increased by inflammatory chemokines, such as CCL2 (5, 6). As CCL2 is highly expressed in the colon of animals treated with AOM/DSS (29), we wondered whether its expression could affect US28 activity in vivo. To test this hypothesis, we generated mice that expressed mouse CCL2 in IECs under control of the villin promoter (*VCCL2* mice). Mouse CCL2, similar to human CCL2, binds to US28 with high affinity (4 nM and 1 nM respectively; Supplemental Figure 1; supplemental material available online with this article; doi:10.1172/JCI42563DS1).

Five *VCCL2* founder mice were obtained from injection of the VCCL2 transgene into fertilized mouse eggs, and 2 lines were derived from them. *VCCL2* mice (line 12) were crossed with *VS28*^{L18} mice to generate *V2S28* mice (Figure 8A). Next, we examined expression of CCL2 and US28 in the intestine of WT, *VCCL2*, and *VS28*^{L18} mice by qPCR. As shown in Figure 8B, *CCL2* mRNA was not detected in the intestine of WT or *VS28* mice. However, *CCL2* mRNA could be readily detected in the intestine of *VCCL2* and *V2S28* mice. *US28* mRNA was only detected in the intestine of *VS28*^{L18} and *V2S28* mice. To analyze the impact of CCL2 expression in the phenotype induced by US28, we examined H&E-stained histological sections (Figure 8, C–E). The intestine of *VCCL2* mice appeared unremarkable, whereas that of the *VS28*^{L18} mice had minor changes as described above. However, in *V2S28* mice, the epithelium was hyperplastic, and the crypts appeared enlarged and resembled those of *VS28*^{L19} and *VS28*^{L36} mice, as shown in Figure 2. Quantification of villus/crypt ratios showed that, compared with WT, *VCCL2* and *VS28*^{L18} littermates, *V2S28* mice had a decreased villus/crypt ratio (ratios of 4.9 ± 0.2, 5.5 ± 0.3, 5.4 ± 0.5, and 3.1 ± 0.2, respectively, n = 4–10). Thus, coexpression of CCL2 augmented the morphological changes induced by US28. To test whether CCL2 affected the increased cellular proliferation promoted by US28, we performed BrdU incorporation experiments as described above. The number of cells incorporating BrdU was similar between WT and *VCCL2* mice. The number of BrdU$^+$ cells was significantly increased in *VS28*^{L18} mice and significantly increased in *V2S28* mice compared with all other groups (Figure 8F). Importantly, after 38 weeks of age, 20% of the *V2S28* mice spontaneously developed jejunal adenomas (P < 0.05 compared with WT), whereas none of the single transgenic littermates examined developed neoplasia (Figure 8G and Table 2). Together, these results indicate that coexpression of CCL2 magnified the changes induced by US28.

Discussion

We show here that US28, a chemokine receptor encoded by CMV, has the ability to induce the development of cancer in transgenic mice. To our knowledge, this is the first report directly linking a specific gene encoded by CMV with development of cancer in transgenic animals.

Table 2
Prevalence of neoplasms in *V2S28* mice

Mice	Age (wk)	Adenoma	Multiplicity
WT	38–45	(0/36) 0%	N/A
VS28^{L18}	38–43	(0/7) 0%	N/A
V2S28	38–44	(2/10) 20%^{A}	1

V2S28 mice were examined for the presence of intestinal neoplasia and compared with littermates. $^{A}P < 0.05$ vs. WT.

Infectious agents account for 18.6% of all cancers (30). Specific agents, such as *Helicobacter pylori*, human papillomavirus, Epstein-Barr virus, and JC virus, have been directly implicated in the etiopathogenesis of several tumors, including gastrointestinal cancers (31, 32).

CMV has also been linked to various cancers (1, 33–36). The CMV genome and antigens have been detected in malignant glioma, EBV-negative Hodgkin lymphoma, cervical cancer, prostatic intraepithelial neoplasia, and prostatic carcinoma. Moreover, active CMV infection has been demonstrated by EM in several of these tumors (1).

CMV DNA (34, 37, 38) or CMV antigens (34, 39) have been detected in colon tumors and in cell lines derived from them, but this association has not been universally confirmed (40–46), perhaps due to the different sensitivities of the methods used for detection of CMV in the different studies (41, 43, 47, 48). Several reports have shown that CMV infection may interfere with key cellular signaling pathways, leading to enhanced survival and angiogenesis, and that it may also alter cell motility and adhesion (49). Following CMV infection, the expression of several protooncogenes is rapidly upregulated (50). Thus, CMV-activated gene transcription may dysregulate various cellular physiological processes that control the cell cycle (35). However, evidence directly linking CMV to cancer is lacking.

Our study does not directly implicate CMV in intestinal cancer in humans, but it demonstrates that a constitutively active chemokine receptor encoded by CMV can promote significant cellular changes in the epithelium that result in dysplasia and cancer in mice. Our results suggest that US28 may do so by interfering with the Wnt pathway. Several studies indicate that activating mutations in the Wnt pathway are the cause of approximately 90% of colorectal cancers (51). These activating mutations lead to increased levels of β-catenin protein by preventing the formation of the β-catenin destruction complex. Stabilized β-catenin translocates to the nucleus and associates with TCF/LEF transcription factors to activate the transcription of Wnt target genes, such as *Birc5* and *Ccnd1*, which affect cell proliferation. We show here that the levels of β-catenin were increased in IECs of *VS28* mice, that β-catenin was found in the nuclei in the adenomas of *VS28* mice, and that these changes were associated with increased expression of cyclin-D1 and with ectopic location of survivin, changes also reported in intestinal cancer (52, 53). Taken together, these results suggest that the increased levels of β-catenin protein in the IECs of *VS28* mice could be the basis for the US28-induced neoplasia.

How could US28 expression affect the levels of β-catenin in IECs? Under normal conditions, β-catenin is present in the cytoplasm within a destruction complex, with GSK-3β, axin, and APC. Within this complex, GSK-3β phosphorylates β-catenin, triggering its ubiquitination and subsequent degradation. We show here that the levels of phosphorylated (inactive) GSK-3β and active β-catenin are increased in IECs from *VS28* mice. These findings suggest that US28 regulates the levels of active β-catenin protein through inactivation of GSK-3β. It is unclear, however, how expression of US28 promotes phosphorylation and inactivation of GSK-3β. A potential mechanism could involve activation of the PI3K/Akt or PLCβ/PKC kinases by US28, as shown for other GPCRs, such as the α-adrenergic receptor and CXCR4 (53). Alternatively, US28 could dimerize with other GPCRs (including Wnt receptors) and promote inactivation of GSK-3β.

Mice that have Wnt pathway activating mutations develop benign adenomas but not cancers (54). Thus, it is surprising that 2 out of the 17 neoplasms found in the *VS28* mice were cancerous. The precise reason for the development of cancer is not clear, but this finding suggests activation of additional oncogenic pathways, such as the MAPK pathway, which has been shown to be important in the progression of colorectal cancer (22, 55). As US28 activates the MAPK pathway both in vitro (26) and in vivo (this study), it is possible that this pathway may also be relevant for the phenotypes observed here.

Our results suggest that US28 shares biological activities with ORF74, the GPCR encoded by HHV-8. Both US28 and ORF74 are constitutively active chemokine receptors. The activity of these receptors can be further modulated by chemokines. Similar to ORF74, US28 promotes increased cell proliferation in vitro and in vivo and induces neoplasia (56). Expression of ORF74 in endothelial progenitor cells of transgenic mice induces development of angioproliferative lesions and tumors that strongly resemble those seen in Kaposi sarcoma (57, 58), whereas expression of US28 in the epithelial cells of the intestine induces development of intestinal neoplasia. At this point it is unclear which cell type in the epithelium accounts for the generation of the phenotype. The intestinal epithelium is comprised of many cell types that can potentially be targeted by the villin promoter used in this study. Among these cells are stem cells present at the bottom of the crypts. Recent work has suggested that such stem cells are the cells of origin of intestinal cancer (59). Specific deletion of the adenomatous polyposis coli (*APC*) gene in Lgr5^{+} stem cells located at the bottom of the crypts leads to development of cancer (59). We show here that US28 is expressed by stem cells present in the crypts of *VS28* mice, and we suggest that US28 expression in the stem cell compartment contributes to the phenotypes observed.

Patients with prolonged inflammatory bowel disease (IBD) have an increased risk of developing colon cancer (60). We speculate that immunosuppressive therapy used to treat such patients may favor reactivation of CMV and promote infection of stem cells. If such stem cells are genetically predisposed, infection by CMV could tip the balance toward dysplasia. This may be accentuated by the expression of inflammatory chemokines that can modulate the activity of US28.

We show here for the first time to our knowledge that the ability of US28 to induce neoplasia can be augmented by coexpression of one of its ligands, CCL2. CCL2 is a chemokine that is expressed in many inflammatory conditions, including IBD (61–63), and that has been shown to directly enhance US28 signaling in vitro (64). Our results suggest that CCL2 may indeed have such properties in vivo. The changes observed in the *V2S28* mice may derive from direct activation of US28 signaling by CCL2, since we have not seen changes in cell proliferation or spontaneous development of neoplasia in *VCCL2* mice even after 1 year of age. However, we

cannot rule out that myeloid cells contribute to the development of the phenotypes elicited by US28 expression.

It is intriguing that both HHV-5 and HHV-8 encode GPCRs that can induce the development of neoplasia and that the activity of these GPCRs can be modulated by chemokines produced during inflammation. A better understanding of the life cycle of herpesviruses in vivo and their target cells and the conditions that facilitate the expression of these constitutively active chemokine receptors will certainly shed light on their role in cancer pathogenesis.

In conclusion, we showed that in vivo expression of the CMV-encoded chemokine receptor US28 in IECs promotes the development of intestinal neoplasia. CMV infects a broad spectrum of cells in the gastrointestinal tract, including epithelial cells (16). The finding that a CMV-encoded gene induces development of intestinal neoplasia in mice should provide a rationale for an extended analysis of the association between CMV and intestinal cancer in humans.

Methods

Mice. The cDNA of the HHV-5–encoded US28 protein (VHL/E strain) was cloned into a pBS-Villin vector that contains the mouse villin promoter (21). The pBS-Villin/US28 plasmid was verified by sequencing, and the transgene was isolated from the plasmid by restriction enzyme digestion and gel purification. To generate *VS28* mice, the transgene was microinjected into C57BL/6J mouse eggs (The Jackson Laboratory), and the resulting founders and their progeny were genotyped by PCR amplification of tail DNA using the following primers: 5′-AGGCCTGCCTTTTCAGTATT-3′ and 5′-CAAGCACGACCGCTATAAGT-3′. To generate transgenic mice expressing CCL2 in the intestinal epithelium (*VCCL2* mice), we cloned a segment of murine genomic DNA encoding CCL2 (65) into the pBS-Villin vector. Founders and progeny were screened using the following primers: 5′-AAGCCAGTTTCCCTTCTTCC-3′ and 5′-TGTCTGGACCCATTCCTTCT-3′. *LGR5* mice were previously described (20). All experiments were performed in accordance with the guidelines of and with the approval of the Animal Care and Use Committee of Mount Sinai School of Medicine.

Histology and immunohistochemistry. Organs were dissected, fixed in 10% phosphate-buffered formalin, and then processed for paraffin sections. Five-μm sections were dewaxed by immersion in xylene (twice for 5 minutes each time) and hydrated by serial immersion in 100%, 90%, 80%, and 70% ethanol and PBS. Antigen retrieval was performed by microwaving sections for 20 minutes in Target Retrieval Solution (DAKO). Sections were washed with PBS (twice for 10 minutes each time), and blocking buffer (10% BSA in TBS) was added for 1 hour. Sections were incubated with primary antibody in blocking buffer overnight at 4°C and then incubated with Alexa Fluor 488–labeled goat anti-rat antibody (1:400; Molecular Probes), Alexa Fluor 594–labeled anti-rabbit antibody (1:400; Molecular Probes), or DyLight 488–labeled donkey anti-chicken antibody (1:400; Jackson) for 30 minutes. Other antibodies were obtained from Abcam (1:200, Ki67; 1:75, pan-keratin; 1:500, GFP) or Cell Signaling Technology (1:25, cyclin-D1; 1:400, survivin; 1:25, β-catenin). Colocalization was performed with ImageJ (http://rsbweb.nih.gov/ij/) and the colocalization finder plug-in (66).

Generation of a rabbit antiserum against US28. A synthetic peptide corresponding to the C-terminal 17 amino acids of the US28 protein (H_2N-SSDTLSDEVCRVSQIIP-CO_2H) was coupled to keyhole limpet hemocyanin through the N-terminal amino group and used to immunize rabbits to generate polyclonal antisera. The specificity of the antisera was assessed by immunoprecipitation followed by Western blotting and immunofluorescence.

Isolation of IECs. Intestines were cut into 2-cm pieces and washed in ice-cold HBSS/10% NCS. The intestinal pieces were incubated in HBSS/5% NCS containing 1 mM DTT for 20 minutes at 37°C. To release the IECs, the pieces were incubated in PBS containing 1.3 mM EDTA for 1 hour at 4°C. After vigorous shaking, IECs were collected and used to prepare RNA, membranes, or protein. To obtain Lgr5$^+$ cells, we incubated intestinal segments from *LGR5* mice (20) and *LGR5S28* mice with DMEM/20% FBS containing dispase II (1 mg/ml) for 20 minutes at 37°C and sorted GFP$^+$ cells on a FACSAria II cell sorter (Becton Dickinson).

IEC proliferation. IECs were isolated 90 minutes after i.p. injection with 2.5 mg BrdU and incubated in DMEM/20% FBS containing dispase II (1 mg/ml) for 20 minutes at 37°C. Cell proliferation was assessed according to the manufacturer's protocol (BD Biosciences).

RNA extraction and qPCR. Total RNA was extracted using the RNeasy Mini Kit (Qiagen) according to the manufacturer's protocol. Reverse transcription was performed using 3 μg total RNA. qPCR was conducted in triplicates using SYBR Green (Applied Biosystems). Relative expression levels were calculated as $2^{(Ct\ Ubiquitin\ -\ Ct\ gene)}$. Primers were designed using Primer Express 2.0 software (Applied Biosystems). The following primers were used: US28 (5′-GCAGCTGCGAGTTCGAAAA-3′, 5′-GCGAGTGACTCGGTCAAGATG-3′), GFP (5′-GTAAACGGCCACAAGTTCAG-3′, 5′-GTCTTGTAGTTGCCGTCGTC-3′), β-catenin (*Ctnnb1*, 5′-GCCCTTTGCCCAGCAAAT-3′, 5′-AGCTGAACTAGTCGTGGAATAGCA-3′), c-Myc (*Myc*, 5′-CGGCGGTGGCAACTTC-3′, 5′-CCTCCAAGTAACTCGGTCATCAT-3′), Survivin (*Birc5*, 5′-GCGGAGGCTGGCTTCA-3′, 5′-AAAAAACACTGGGCCAAATCA-3′), Cyclin-D1 (*Ccnd1*, 5′-TCCGCAAGCATGCACAGA-3′, 5′-GGTGGGTTGGAAATGAACTTCA-3′), and CCL2 (5′-GCTGGAGCATCCACGTGTT-3′, 5′-ATCTTGCTGGTGAATGAGTAGCA-3′).

US28 receptor binding. Membranes of IECs were prepared as previously described (67). Cell membranes (~0.3 mg protein) were homogenized for 2 seconds by sonication and incubated with 50 pM [^{125}I]CCL5 in binding buffer (50 mM HEPES, pH 7.4, 1 mM $CaCl_2$, 5 mM $MgCl_2$, and 100 mM NaCl) at 37°C for 1 hour. The reaction was terminated by filtration over GF/B filters presoaked in 0.3% PEI, followed by 3 rapid washes with ice-cold binding buffer. Radioactivity was quantified with a gamma counter. Specific binding was defined as total binding minus nonspecific binding determined with 0.1 μM CX_3CL1 as a competing ligand. Protein concentrations were determined spectrophotometrically with the BCA Kit (Pierce), with BSA as a standard.

Western blot. Isolated IECs were lysed in RIPA buffer (Invitrogen) containing protease inhibitors (Roche) and phosphatase inhibitors (Pierce), sonicated, separated by SDS (10%) gel electrophoresis, and blotted onto a PVDF membrane. The membrane was blocked for 60 minutes at room temperature in TBS (Boston Bioproducts) buffer containing 0.05% Tween and 5% (v/w) milk powder. Subsequently, anti–β-catenin, Phospho-ERK1/2, ERK1/2, cyclin-D1, Survivin, Phospho–GSK-3β/Ser^9, or anti–β-actin antibodies (all 1:1,000, Cell Signaling Technology) or anti-ABC antibody (clone 8E7, 1:2,000, Millipore) were incubated for 1 hour at 22°C in TBS containing 0.05% Tween (T-TBS) and 5% (v/w) milk powder, used in combination with a rabbit anti-goat HRP-conjugated secondary antibody (1:2,000), and incubated for 60 minutes at room temperature in T-TBS containing 5% (v/w) milk powder. Immunoreactivity was detected by an ECL assay.

AOM/DSS model. *VS28* mice and WT littermates were injected with AOM (12 mg/kg; Sigma-Aldrich), and after 2 weeks, they were subjected to 3 rounds of 2.5% DSS (MW = 36.000–50.000; MP Biomedicals) in the drinking water. At sacrifice, the colon was cut open longitudinally, briefly stained with methylene blue (0.2% [v/v]), and high-resolution digital pictures were obtained of the mucosa using a dissecting microscope. Neoplastic lesions were counted and tumor area was determined from digital pictures using ImageJ 1.41 (http://rsbweb.nih.gov/ij/).

Statistics. Statistical analyses were performed using GraphPad Prism (GraphPad Software). Differences among means were evaluated by a

2-tailed *t* test, ANOVA followed by Dunnett's post-test, or a 2 × 2 contingency table using Fisher's exact test. $P < 0.05$ was considered significant. All results shown represent mean ± SEM.

Acknowledgments

We thank Andrea Martin for technical help, Steven Itzkowitz for critical comments, Kevin Haigis for help importing the *Lgr5-EGFP-IRES-creERT2* mice, and Jenny and Jon Steingart and Jenna and Paul Segal for a grant supporting G. Bongers. This work was supported by grants from the NIH (P01 DK072201 to S.A. Lira and L. Mayer) and UK Medical Research Council (to A. Fraile-Ramos).

Received for publication February 4, 2010, and accepted in revised form August 25, 2010.

Address correspondence to: Sergio A. Lira, Immunology Institute, Mount Sinai School of Medicine, 1425 Madison Ave., Box 1630, New York, New York 10029-6574, USA. Phone: 212.659.9404; Fax: 212.849.2525; E-mail: sergio.lira@mssm.edu.

Alberto Fraile-Ramos's present address is: Cell Biology of Herpesvirus Laboratory, Centro Nacional de Biotecnología, Consejo Superior de Investigaciones Científicas, Campus Universidad Autonoma, Madrid 28049, Spain.

1. Soderberg-Naucler C. Does cytomegalovirus play a causative role in the development of various inflammatory diseases and cancer? *J Intern Med*. 2006; 259(3):219–246.
2. Mocarski ES, Shenk T, Pass RF. Cytomegaloviruses. In: Knipe DM, ed. *Fields Virology*. Philadelphia, Pennsylvania, USA: Lippincott, Williams, and Wilkins; 2006: 2701–2772.
3. Maussang D, Vischer HF, Leurs R, Smit MJ. Herpesvirus-encoded G protein-coupled receptors as modulators of cellular function. *Mol Pharmacol*. 2009; 76(4):692–701.
4. Neote K, DiGregorio D, Mak JY, Horuk R, Schall TJ. Molecular cloning, functional expression, and signaling characteristics of a C-C chemokine receptor. *Cell*. 1993;72(3):415–425.
5. Kledal TN, Rosenkilde M, Schwartz TW. Selective recognition of the membrane-bound CX3C chemokine, fractalkine, by the human cytomegalovirus-encoded broad-spectrum receptor US28. *FEBS Lett*. 1998;441(2):209–214.
6. Kuhn DE, Beall CJ, Kolattukudy PE. The cytomegalovirus US28 protein binds multiple CC chemokines with high affinity. *Biochem Biophys Res Commun*. 1995;211(1):325–330.
7. Vischer HF, Leurs R, Smit MJ. HCMV-encoded G-protein-coupled receptors as constitutively active modulators of cellular signaling networks. *Trends Pharmacol Sci*. 2006;27(1):56–63.
8. Casarosa P, et al. Constitutive signaling of the human cytomegalovirus-encoded chemokine receptor US28. *J Biol Chem*. 2001;276(2):1133–1137.
9. Beisser PS, Laurent L, Virelizier JL, Michelson S. Human cytomegalovirus chemokine receptor gene US28 is transcribed in latently infected THP-1 monocytes. *J Virol*. 2001;75(13):5949–5957.
10. Zipeto D, Bodaghi B, Laurent L, Virelizier JL, Michelson S. Kinetics of transcription of human cytomegalovirus chemokine receptor US28 in different cell types. *J Gen Virol*. 1999;80(pt 3):543–547.
11. Bodaghi B, et al. Chemokine sequestration by viral chemoreceptors as a novel viral escape strategy: withdrawal of chemokines from the environment of cytomegalovirus-infected cells. *J Exp Med*. 1998; 188(5):855–866.
12. Randolph-Habecker JR, et al. The expression of the cytomegalovirus chemokine receptor homolog US28 sequesters biologically active CC chemokines and alters IL-8 production. *Cytokine*. 2002;19(1):37–46.
13. Haskell CA, Cleary MD, Charo IF. Unique role of the chemokine domain of fractalkine in cell capture. Kinetics of receptor dissociation correlate with cell adhesion. *J Biol Chem*. 2000;275(44):34183–34189.
14. Pleskoff O, et al. The human cytomegalovirus-encoded chemokine receptor US28 induces caspase-dependent apoptosis. *FEBS J*. 2005;272(16):4163–4177.
15. Maussang D, et al. Human cytomegalovirus-encoded chemokine receptor US28 promotes tumorigenesis. *Proc Natl Acad Sci U S A*. 2006;103(35):13068–13073.
16. Sinzger C, Grefte A, Plachter B, Gouw AS, The TH, Jahn G. Fibroblasts, epithelial cells, endothelial cells and smooth muscle cells are major targets of human cytomegalovirus infection in lung and gastrointestinal tissues. *J Gen Virol*. 1995;76(pt 4):741–750.
17. Rene E, et al. Cytomegalovirus colitis in patients with acquired immunodeficiency syndrome. *Dig Dis Sci*. 1988;33(6):741–750.
18. Landolfo S, Gariglio M, Gribaudo G, Lembo D. The human cytomegalovirus. *Pharmacol Ther*. 2003; 98(3):269–297.
19. Maiorana A, Baccarini P, Foroni M, Bellini N, Giusti F. Human cytomegalovirus infection of the gastrointestinal tract in apparently immunocompetent patients. *Hum Pathol*. 2003;34(12):1331–1336.
20. Barker N, et al. Identification of stem cells in small intestine and colon by marker gene Lgr5. *Nature*. 2007;449(7165):1003–1007.
21. Pinto D, Robine S, Jaisser F, El Marjou FE, Louvard D. Regulatory sequences of the mouse villin gene that efficiently drive transgenic expression in immature and differentiated epithelial cells of small and large intestines. *J Biol Chem*. 1999;274(10):6476–6482.
22. Fang JY, Richardson BC. The MAPK signalling pathways and colorectal cancer. *Lancet Oncol*. 2005; 6(5):322–327.
23. Scoville DH, Sato T, He XC, Li L. Current view: intestinal stem cells and signaling. *Gastroenterology*. 2008; 134(3):849–864.
24. Wodarz A, Nusse R. Mechanisms of Wnt signaling in development. *Annu Rev Cell Dev Biol*. 1998;14:59–88.
25. Shevtsov SP, Haq S, Force T. Activation of beta-catenin signaling pathways by classical G-protein-coupled receptors: mechanisms and consequences in cycling and non-cycling cells. *Cell Cycle*. 2006; 5(20):2295–2300.
26. Maussang D, et al. The human cytomegalovirus-encoded chemokine receptor US28 promotes angiogenesis and tumor formation via cyclooxygenase-2. *Cancer Research*. 2009;69(7):2861–2869.
27. Reya T, Clevers H. Wnt signalling in stem cells and cancer. *Nature*. 2005;434(7035):843–850.
28. Neufert C, Becker C, Neurath M. An inducible mouse model of colon carcinogenesis for the analysis of sporadic and inflammation-driven tumor progression. *Nat Protoc*. 2007;2(8):1998–2004.
29. Tokuyama H, et al. The simultaneous blockade of chemokine receptors CCR2, CCR5 and CXCR3 by a non-peptide chemokine receptor antagonist protects mice from dextran sodium sulfate-mediated colitis. *Int Immunol*. 2005;17(8):1023–1034.
30. Zur Hausen H. The search for infectious causes of human cancers: where and why. *Virology*. 2009; 392(1):1–10.
31. Selgrad M, Malfertheiner P, Fini L, Goel A, Boland CR, Ricciardiello L. The role of viral and bacterial pathogens in gastrointestinal cancer. *J Cell Physiol*. 2008;216(2):378–388.
32. White MK, Khalili K. Expression of JC virus regulatory proteins in human cancer: potential mechanisms for tumourigenesis. *Eur J Cancer*. 2005; 41(16):2537–2548.
33. Harkins L, et al. Specific localisation of human cytomegalovirus nucleic acids and proteins in human colorectal cancer. *Lancet*. 2002;360(9345):1557–1563.
34. Cobbs CS, et al. Human cytomegalovirus infection and expression in human malignant glioma. *Cancer Res*. 2002;62(12):3347–3350.
35. Michaelis M, Doerr HW, Cinatl J. The story of human cytomegalovirus and cancer: increasing evidence and open questions. *Neoplasia*. 2009;11(1):1–9.
36. Prins RM, Cloughesy TF, Liau LM. Cytomegalovirus immunity after vaccination with autologous glioblastoma lysate. *N Engl J Med*. 2008;359(5):539–541.
37. Huang ES, Roche JK. Cytomegalovirus D.N.A. and adenocarcinoma of the colon: Evidence for latent viral infection. *Lancet*. 1978;1(8071):957–960.
38. Mariguela VC, Chacha SG, Cunha Ade A, Troncon LE, Zucoloto S, Figueiredo LT. Cytomegalovirus in colorectal cancer and idiopathic ulcerative colitis. *Rev Inst Med Trop Sao Paulo*. 2008;50(2):83–87.
39. Hashiro GM, Horikami S, Loh PC. Cytomegalovirus isolations from cell cultures of human adenocarcinomas of the colon. *Intervirology*. 1979;12(2):84–88.
40. Brichacek B, Hirsch I, Zavadova H, Prochazka M, Faltyn J, Vonka V. Absence of cytomegalovirus DNA from adenocarcinoma of the colon. *Intervirology*. 1980;14(3–4):223–227.
41. Roche JK, Cheung KS, Boldogh I, Huang ES, Lang DJ. Cytomegalovirus: detection in human colonic and circulating mononuclear cells in association with gastrointestinal disease. *Int J Cancer*. 1981; 27(5):659–667.
42. Hart H, Neill WA, Norval M. Lack of association of cytomegalovirus with adenocarcinoma of the colon. *Gut*. 1982;23(1):21–30.
43. Grail A, Norval M. Elution of cytomegalovirus antibodies from adenocarcinoma of the colon. *Gut*. 1985; 26(10):1053–1058.
44. Ruger R, Fleckenstein B. Cytomegalovirus DNA in colorectal carcinoma tissues. *Klin Wochenschr*. 1985;63(9):405–408.
45. Knösel T, Schewe C, Dietel M, Petersen I. Cytomegalovirus is not associated with progression and metastasis of colorectal cancer. *Cancer Lett*. 2004; 211(2):243–247.
46. Akintola-Ogunremi O, Luo Q, He TC, Wang HL. Is cytomegalovirus associated with human colorectal tumorigenesis? *Am J Clin Pathol*. 2005;123(2):244–249.
47. Avni A, et al. Antibody pattern to human cytomegalovirus in patients with adenocarcinoma of the colon. *Intervirology*. 1981;16(4):244–249.
48. Scheurer ME, El-Zein R, Bondy ML, Harkins L, Cobbs CS. RE: "Lack of association of herpesviruses with brain tumors". *J Neurovirol*. 2007;13(1):85; author reply 86–87.
49. Cinatl J Jr, Vogel JU, Kotchetkov R, Wilhelm Doerr H. Oncomodulatory signals by regulatory proteins encoded by human cytomegalovirus: a novel role for viral infection in tumor progression. *FEMS Microbiol Rev*. 2004;28(1):59–77.
50. Boldogh I, AbuBakar S, Albrecht T. Activation of proto-oncogenes: an immediate early event in human cytomegalovirus infection. *Science*. 1990;

247(4942):561–564.
51. Giles RH, van Es JH, Clevers H. Caught up in a Wnt storm: Wnt signaling in cancer. *Biochim Biophys Acta*. 2003;1653(1):1–24.
52. Pennati M, Folini M, Zaffaroni N. Targeting survivin in cancer therapy: fulfilled promises and open questions. *Carcinogenesis*. 2007;28(6):1133–1139.
53. Sheng H, et al. Nuclear translocation of beta-catenin in hereditary and carcinogen-induced intestinal adenomas. *Carcinogenesis*. 1998;19(4):543–549.
54. Taketo MM, Edelmann W. Mouse models of colon cancer. *Gastroenterology*. 2009;136(3):780–798.
55. Trobridge P, et al. TGF-beta receptor inactivation and mutant Kras induce intestinal neoplasms in mice via a beta-catenin-independent pathway. *Gastroenterology*. 2009;136(5):1680–1688.e7.
56. Arvanitakis L, Geras-Raaka E, Varma A, Gershengorn MC, Cesarman E. Human herpesvirus KSHV encodes a constitutively active G-protein-coupled receptor linked to cell proliferation. *Nature*. 1997; 385(6614):347–350.
57. Yang TY, et al. Transgenic expression of the chemokine receptor encoded by human herpesvirus 8 induces an angioproliferative disease resembling Kaposi's sarcoma. *J Exp Med*. 2000;191(3):445–454.
58. Montaner S, et al. Endothelial infection with KSHV genes in vivo reveals that vGPCR initiates Kaposi's sarcomagenesis and can promote the tumorigenic potential of viral latent genes. *Cancer Cell*. 2003;3(1):23–36.
59. Barker N, et al. Crypt stem cells as the cells-of-origin of intestinal cancer. *Nature*. 2009;457(7229):608–611.
60. Ullman T, Croog V, Harpaz N, Sachar D, Itzkowitz S. Progression of flat low-grade dysplasia to advanced neoplasia in patients with ulcerative colitis. *Gastroenterology*. 2003;125(5):1311–1319.
61. Uguccioni M, et al. Increased expression of IP-10, IL-8, MCP-1, and MCP-3 in ulcerative colitis. *Am J Pathol*. 1999;155(2):331–336.
62. Mazzucchelli L, et al. Differential in situ expression of the genes encoding the chemokines MCP-1 and RANTES in human inflammatory bowel disease. *J Pathol*. 1996;178(2):201–206.
63. Reinecker HC, Loh EY, Ringler DJ, Mehta A, Rombeau JL, MacDermott RP. Monocyte-chemoattractant protein 1 gene expression in intestinal epithelial cells and inflammatory bowel disease mucosa. *Gastroenterology*. 1995;108(1):40–50.
64. Gao JL, Murphy PM. Human cytomegalovirus open reading frame US28 encodes a functional beta chemokine receptor. *J Biol Chem*. 1994; 269(46):28539–28542.
65. Grewal IS, et al. Transgenic monocyte chemoattractant protein-1 (MCP-1) in pancreatic islets produces monocyte-rich insulitis without diabetes: abrogation by a second transgene expressing systemic MCP-1. *J Immunol*. 1997;159(1):401–408.
66. Rasband WS. ImageJ. U.S. National Institutes of Health Web site. http://rsb.info.nih.gov/ij/. Accessed August 27, 2010.
67. Bongers G, Leurs R, Robertson J, Raber J. Role of H_3-receptor-mediated signaling in anxiety and cognition in wild-type and Apoe$^{-/-}$ mice. *Neuropsychopharmacology*. 2004;29(3):441–449.